Raman Spectroscopy of the $Ni_5(TeO_3)_4Cl_2$ Single Crystal

A.V. Peschanskii[1], V.P. Gnezdilov[1], A.Yu. Glamazda[1,2]

[1]*B. Verkin Institute for Low Temperature Physics and Engineering of the National Academy of Sciences of Ukraine, 47 Nauky Ave., 61103 Kharkov, Ukraine*

[2]*V.N. Karazin Kharkiv National University, 4 Svobody Sq., 61022, Kharkov, Ukraine*

The two-dimensional quantum spin system $Ni_5(TeO_3)_4Cl_2$ has a clearly pronounced 2D spin structure with the developed Ni^{2+} triangular structure that can give rise to the appearance of the exotic magnetic states. The antiferromagnetic transition was previously revealed in the single crystal at temperature T_N = 28.5 K [1]. Raman spectroscopy is the informative non-destructive method that can probe the interplay of lattice, charge, and spin quantum excitations. In our previous work [2], the main attention was paid to the analysis of the phonon spectrum. In the present work, we focus on the analysis of the revealed Raman peculiarities of the $Ni_5(TeO_3)_4Cl_2$ single crystal.

The crystal $Ni_5(TeO_3)_4Cl_2$ is monoclinic with space group *C2/c* (C_{2h}^6) and Z = 4. The crystal unit cell has a dimension: *a*=19.5674Å, *b*=5.2457Å, *c*=16.3084Å, and *β*=125.29° [3].

Raman spectra of the $Ni_5(TeO_3)_4Cl_2$ single crystal presented in the present work were taken in the frequency region of 3–850 cm⁻¹ in the temperature range of 2-300 K. A_g and B_g modes are active in Raman tensor components: A_g – *XX, YY, ZZ, XY, YX*, B_g – *XZ, ZX YZ, ZY*.

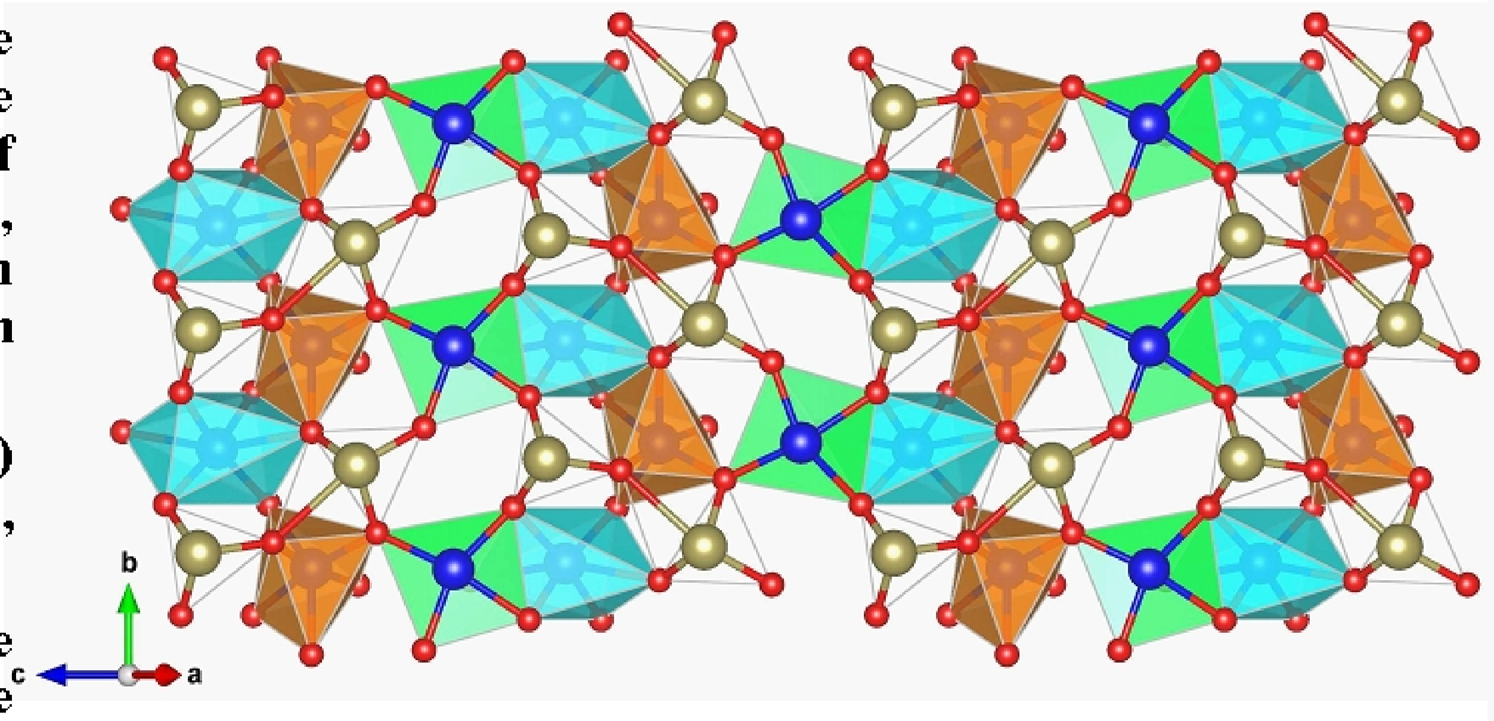

Fig. 1. Ni octahedral shaded layer [1]. Ti atoms are shown in mustard color.

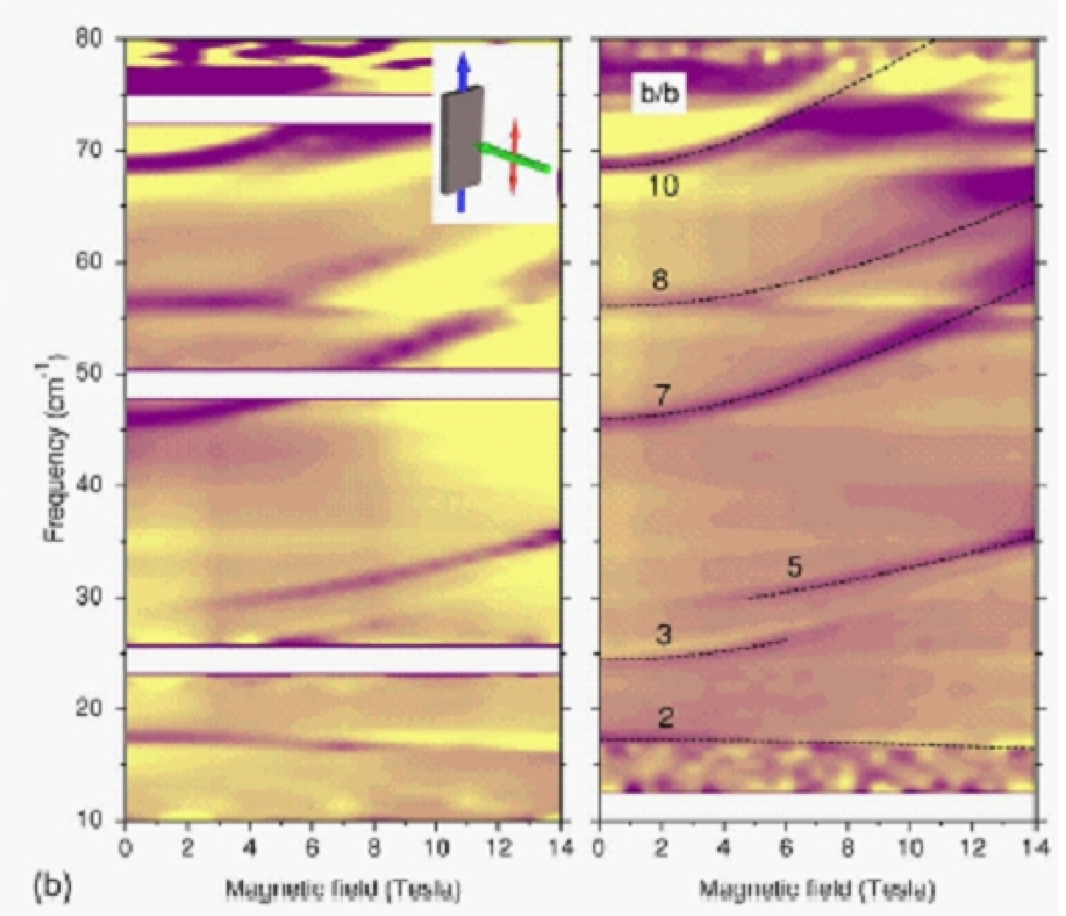

Fig. 2. Spin resonance in the ordered magnetic state of $Ni_5(TeO3)_4Cl_2$ [4].

Previous Raman work [2]

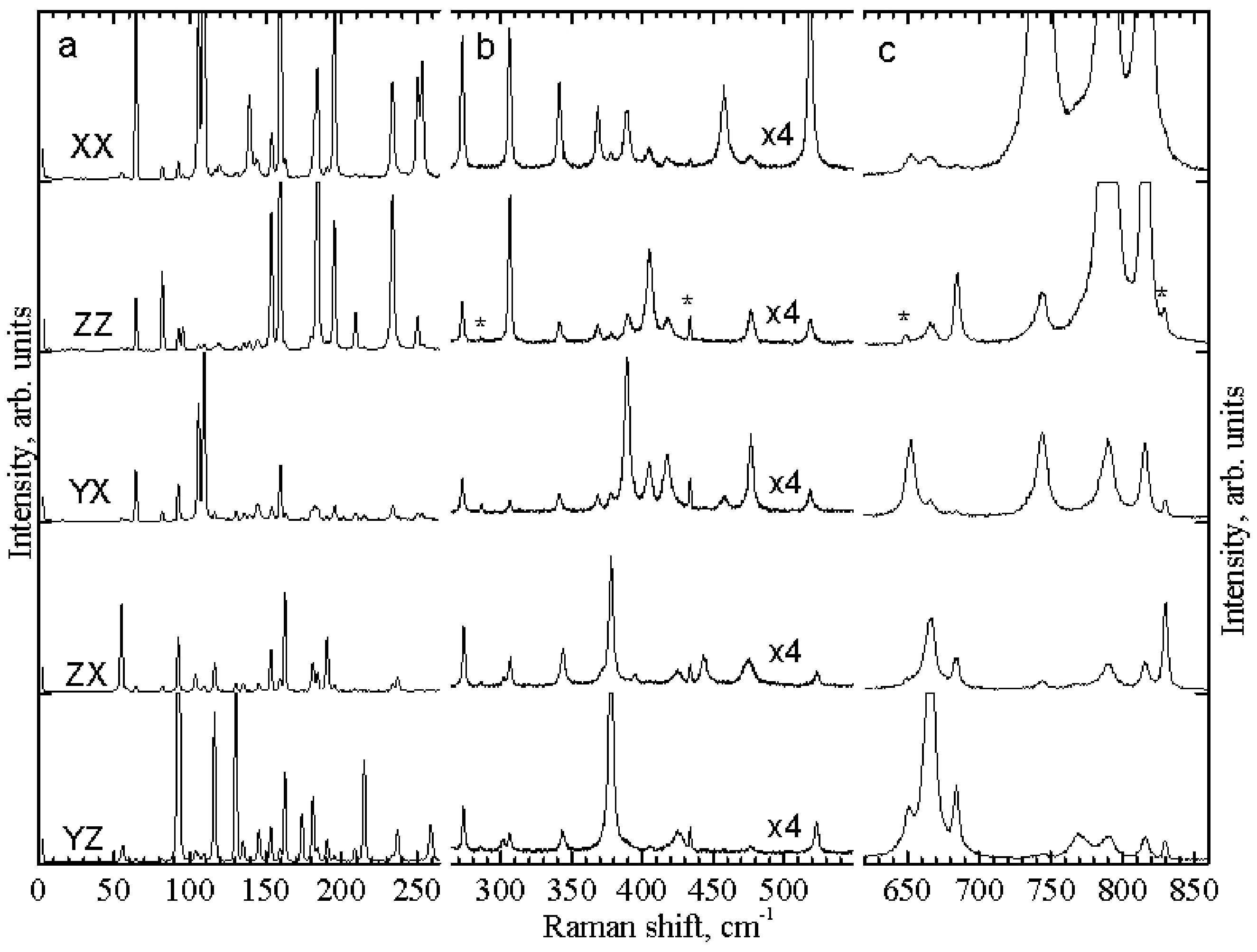

Fig. 3, 4. Raman spectra at 15 K (25 K) [2].

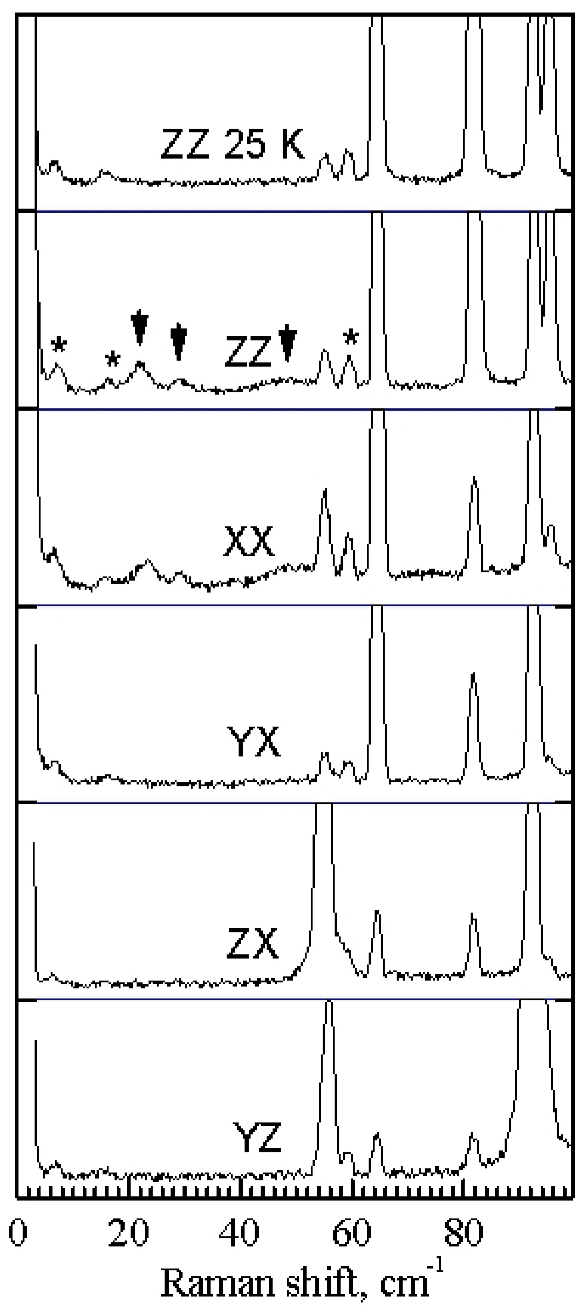

Frequency (cm⁻¹)	Simmery	Experimental scattering geometry		Frequency (cm⁻¹)	Simmery	Experimental scattering geometry	Free TeO_3 unit [10]
55.1	B_g	ZX		253.4	A_g	XX	
64.5	A_g	XX		259.0	B_g	YZ	
81.8	A_g	ZZ		272.8	A_g	XX	
92.5	B_g	YZ		273.8	B_g	ZX, YZ	
95.4	A_g	ZZ		301.8	B_g	ZX	
103.8	B_g	ZX		306.3	A_g	ZZ,XX	ν_4(E) 326
105.8	A_g	ZZ,XX		341.5	A_g	XX	
109.4	A_g	XX, YX		343.8	B_g	YZ	
116.5	B_g	YZ		368.5	A_g	XX	ν_2(A_1) 364
119.6	A_g	XX		377.9	B_g	YZ	
130.5	B_g	YZ		389.3	A_g	XX, YX	
134.8	B_g	YZ		395.0	B_g	ZX	
139.2	A_g	XX		405.0	A_g	ZZ	
144.5	A_g	XX, YX		417.9	A_g	YX	
145.6	B_g	YZ		425.0	B_g	ZX, YZ	
153.5	B_g	ZX, YZ		443.7	B_g	ZX	
153.8	A_g	ZZ		457.9	A_g	XX	
159.7	A_g	ZZ,XX		474.6	B_g	ZX	
162.9	B_g	ZX, YZ		476.8	A_g	YX	
174.0	B_g	YZ		518.8	A_g	XX	
181.4	B_g	YZ		523.2	B_g	YZ	
182.5	A_g	XX		651.1	B_g	YZ	
184.4	A_g	ZZ		652.3	A_g	YX	
190.7	B_g	ZX		666.0	B_g	YZ	ν_3(E) 703
195.4	A_g	ZZ,XX		684.2	B_g	YZ	
209.0	B_g	YZ		684.9	A_g	ZZ	
209.4	A_g	ZZ		743.9	A_g	XX	
215.1	B_g	YZ		770.1	B_g	YZ	
233.7	A_g	ZZ		789.9	A_g	ZZ,XX	ν_1(A_1) 758
237.1	B_g	YZ		815.6	A_g	ZZ,XX	
250.3	A_g	XX		829.9	B_g	ZX	

Γ_{vib}=34A_g + 35B_g + 34A_u+35B_u

34A_g+35B_g modes are Raman active.

In different scattering geometries we observed 62 phonon lines (Table 1) of the 69 predicted ones by theory-group analysis for the monoclinic C_{2h}^6 lattice symmetry [2]. Three additional weak lines with frequencies 22.3, 29.4, and 49.0 cm⁻¹ vanish at around T_N with temperature rising [2].

Referenses:

[1]. R.Becker, M. Prester, H. Berger, M johnsson, D. Drobac, and I. Zivkovic, Sol. State Sci. 9, 223 (2007).

[2]. A.V. Peschanskii, V.P. Gnezdilov, V.I. Fomin, at. al., Ukrainian J. Phys. 54, 205 (2009)

[3]. M. Johnsson, K.W. Tornroos, P. Lemmens, and P. Millet, Chem. Mater. 15, 68 (2003).

[4]. Mihaly, T. Feher, B. Dora, B. Nafradi, H. Berger, and L.Forro, Phys. Rev. B 74, 174403 (2006).

Table 1. Symmetry and frequencies of the phonon modes in $Ni_5(TeO3)_4Cl_2$ [2] at T = 15 K.

New Raman data

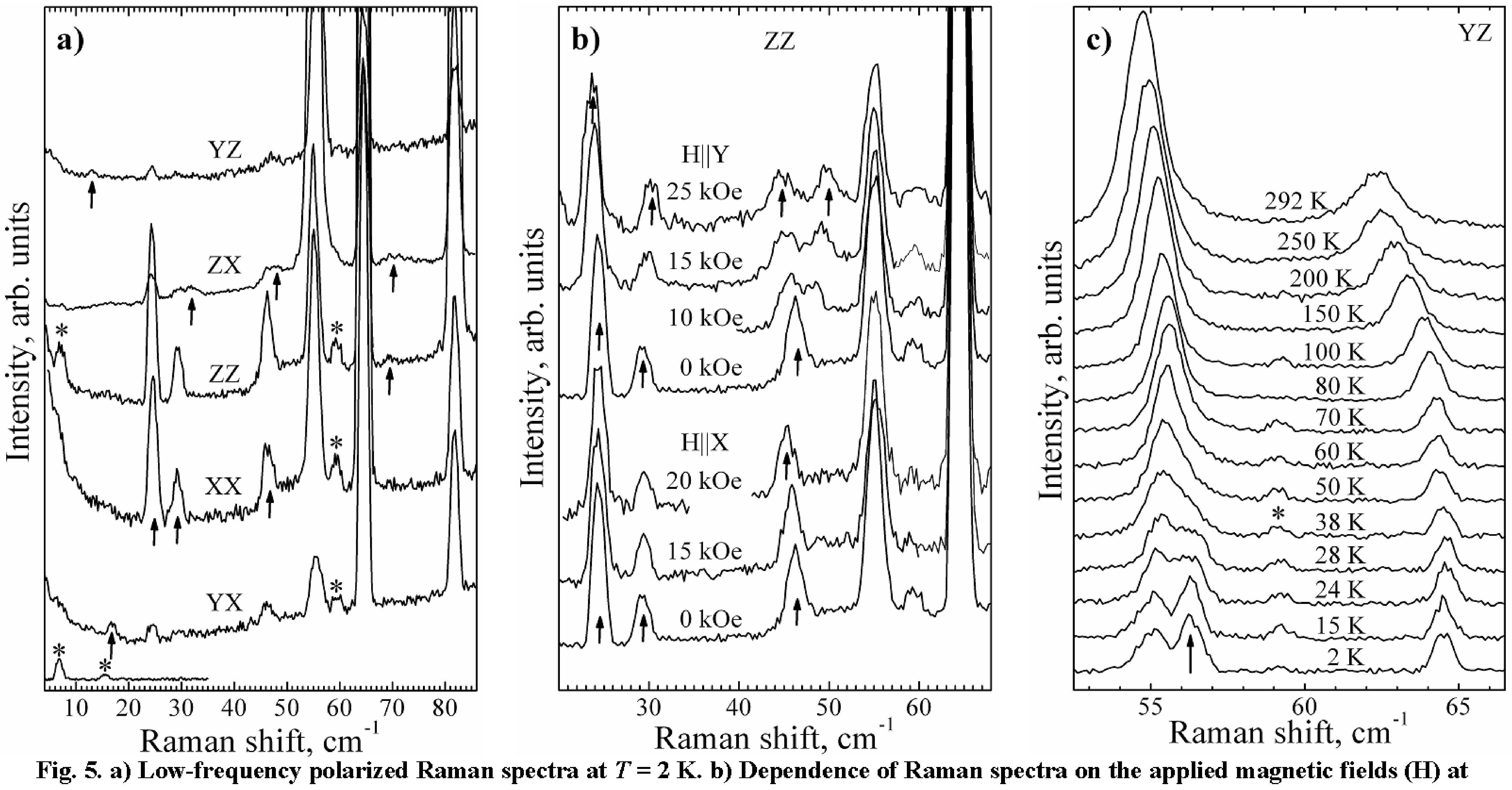

Fig. 5. a) Low-frequency polarized Raman spectra at *T* = 2 K. b) Dependence of Raman spectra on the applied magnetic fields (H) at *T* = 2 K. c) Temperature dependent Raman spectra. Spectral resolution: 1.8 cm⁻¹ (a and b); 0.6 cm⁻¹ (c). The arrows mark additional lines. The asterisks denote the plasma lines of He-Ne laser (λ_{exc}=632.8 nm).

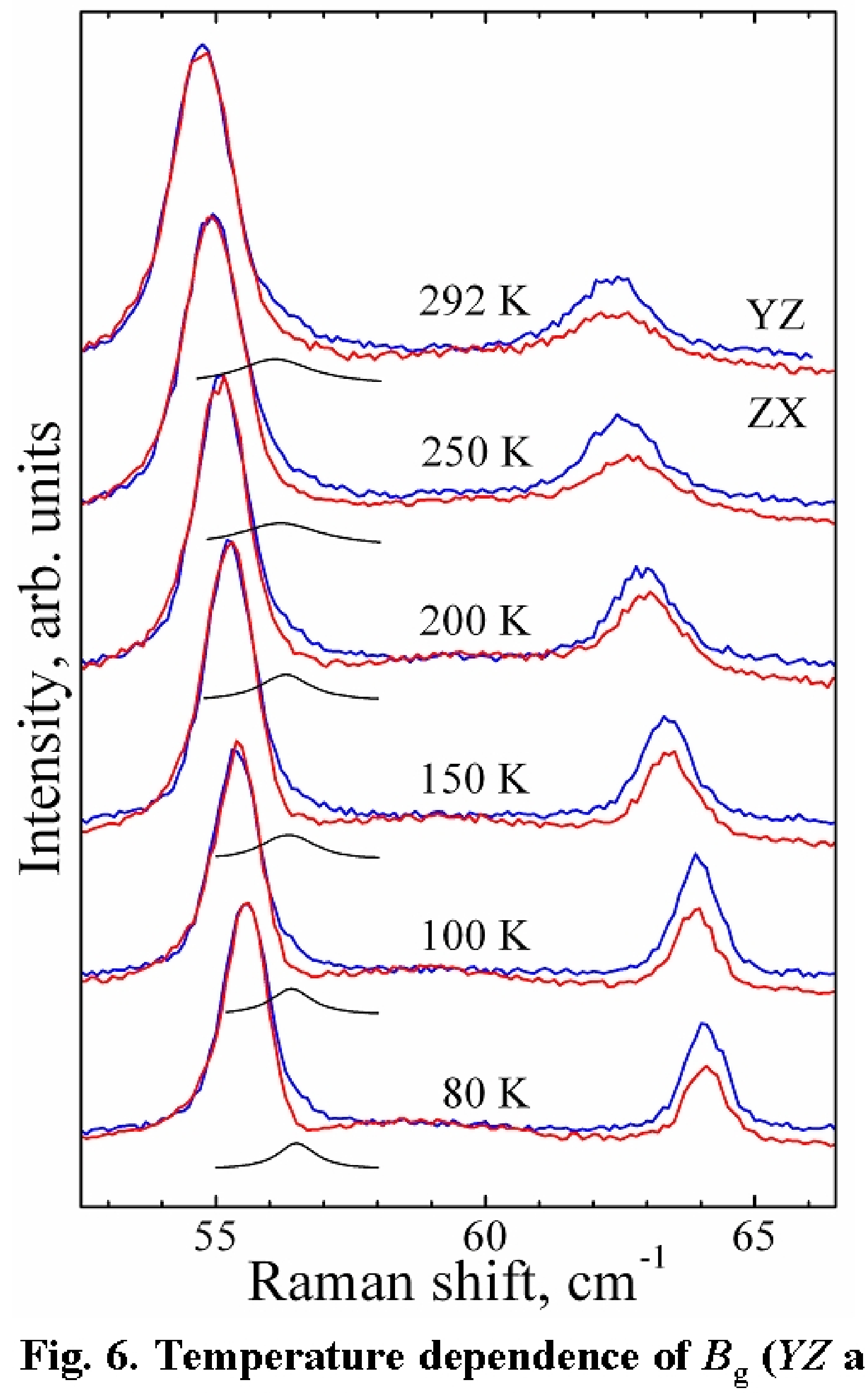

Fig. 6. Temperature dependence of B_g (*YZ* and *ZX*) Raman spectra. Spectral resolution: 0.6 cm⁻¹. λ_{exc} = 632.8 nm.

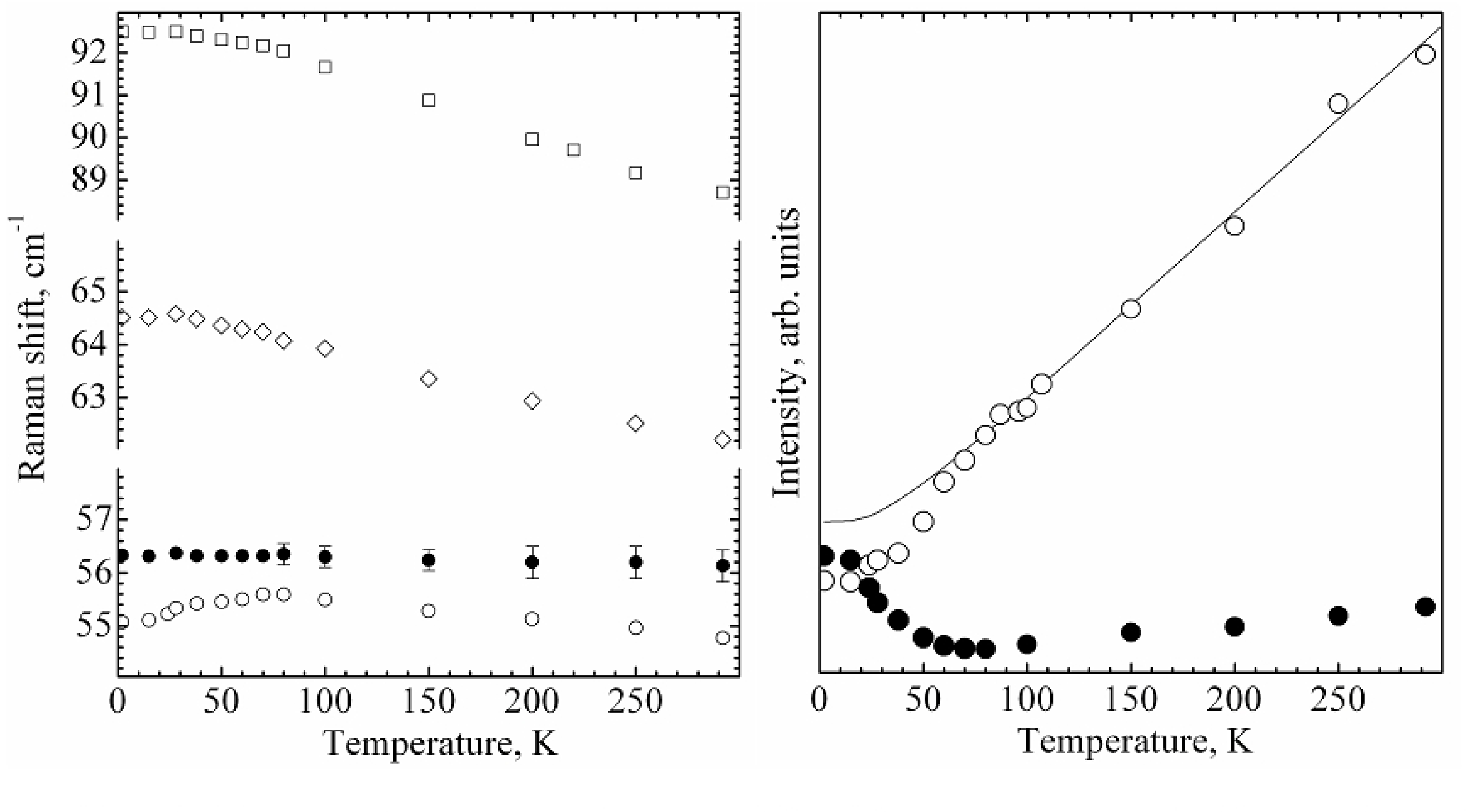

Fig. 7. Temperature dependence of the Raman position (left panel) and intensity (right panel) of the phonon modes: ○ - 55 cm⁻¹, ● - 56.3 cm⁻¹, ◊ - 64.5 cm⁻¹, □ - 92.5 cm⁻¹. The spectral resolution: 0.6 cm⁻¹.

Raman scattering data		FIR (2.5 K) [4]	
Previous work (15 K) [2]	Present work (2 K)	At H = 0	At high field
	13.1±0.5	13.5	
	16.8±0.5	17.3	
22.3±0.5	24.4±0.2	24.4	
			25.5
29.4±0.5	29.2±0.3		29
	31.9±0.4	32.2	
49.0±1.0	46.2±0.2 48.2±0.5	46 46	
56.3±0.1 ?	56.3±0.1 phonon	56	
			63
	69.4±0.4 69.9±0.5	68.5 68.5	
two-magnon	50.0±1.0		

Conclusions

In addition to the phonon lines, weak peaks at 16.8, 24.4, 29.2, 46.2, 69.4 cm⁻¹ (A_g modes) and 13.1, 31.9, 48.2, 69.9 cm⁻¹ (B_g modes) were observed in the spectra at 2 K (Fig. 5a). The energy positions of additional peaks are in good accordance with spin-resonance data [4]. The temperature behavior of these lines is typical for the one-magnon scattering. The evolution of additional peaks has been investigated in applied magnetic field of 0 – 25 kOe in different geometries (Fig. 5b).

We have found that the 56.3 cm⁻¹ line disappears in the spectra at temperatures well above T_N (Fig. 5c, 6) . Besides, this line is not sensitive to the applied magnetic field. Usually such behavior is typical for a two-magnon scattering. However, the temperature dependence of its linewidth (see Fig. 5c) does not allow us to attribute this excitation to either one-magnon or two-magnon. We suppose that this line can be assigned to a phonon excitation.